Published in: J. Mater. Sci., 2001, vol. 36, 5603-5608

THE EFFECT OF HIGH TEMPERATURE EXPOSURE ON DENDRITIC SEGREGATION IN A CONVENTIONALLY CAST NI BASED SUPERALLOY

M.J. Starink* and R.C. Thomson

Institute of Polymer Technology and Materials Engineering,
Loughborough University, Loughborough LE11 3TU, UK

* currently at Materials Research Group, School of Engineering Sciences,
University of Southampton, Southampton S017 1BJ, UK

Abstract

Dendritic segregation in conventionally cast, commercially heat treated and exposed MarM002 turbine blades has been investigated using scanning electron microscopy (SEM) and energy dispersive X-ray analysis (EDS). During casting Cr, Co and W segregate to the dendrites and Hf, Ti and Ta segregate to the eutectics. As a result of the dissolution of γ' precipitates in the dendrites and coarsening of γ' precipitates in the eutectics this segregation aggravates during exposure at 1000ºC. At this high exposure temperature homogenisation of dendritic segregation does not occur because it involves long diffusion distances and a low driving force compared with dissolution and coarsening of γ' precipitates.

1 Introduction

Conventionally cast (CC) nickel based superalloys, like the commercial alloy MarM002, are widely used in the manufacture of industrial gas turbine engine components, as well as in aero gas turbine engines. Solidification of these alloys proceeds via the growth of dendrites (γ phase), which leads to rejection of specific alloying elements to the liquid, i.e. dendritic segregation. At the elevated temperatures at which the alloys operate many microstructure evolution processes can occur, such as MC carbide dissolution and formation of lower carbides [1,2,3,4], dissolution of γ', and homogenisation of the initial dendritic segregation. In order to utilise these nickel-based superalloys effectively, it is necessary to have a thorough understanding of these processes.

Although segregation in several Ni-based superalloys on casting has been investigated [5,6,7,8,9], evolution of the segregation during exposure at the elevated temperatures at which the alloys operate has received very little attention. Hence, an extensive study into the evolution of the microstructure during high temperature exposure of MarM002 alloys has been performed. In the present work, we will especially focus on the evolution of the microsegregation which is investigated using scanning electron microscopy (SEM) and energy dispersive X-ray spectroscopy (EDS). Additionally, the sequence in which the different microstructural processes evolve is investigated.

2 Experimental Methods

Conventionally cast (CC), uncoated MarM002 (nominal composition in mass %: 9% Cr, 10% W, 10% Co, 5.5% Al, 1.5% Ti, 2.5% Ta, 1.5% Hf, 0.06% Zr, 0.01%Mo, 0.15% C, 0.013% B, bal. Ni) blades were given a commercial heat treatment consisting of heating up to 1190 °C and holding for 15 minutes (this is essentially a solutionising treatment), followed by further heat treatment at 870 °C for 18 hours. All samples were air cooled after each heat treatment. This condition will henceforth be referred to as the 'commercially heat treated' (CHT) condition. This condition is essentially that which a new CC blade is in when it is first put in to service. Subsequent heat treatments were performed at 800, 900 and 1000 °C for 6000 h (250 days).

For SEM and optical microscopy, samples were mounted, ground, polished and etched for 5 seconds in Kalling's reagent (40 g $CuCl_2$, 80 ml HCl and 40 ml methanol). (It is noted that this etch will reveal most γ' but may not be suitable to etch the very fine γ' that forms during cooling after heat treatments.) SEM analysis was performed on a Cambridge Instruments Stereoscan 360 operated at 20 kV. In order to reveal dendritic contrast SEM backscattered imaging contrast settings were set close to maximum. An energy dispersive X-ray spectroscopy (EDS) facility attached to the SEM was used for quantitative chemical analyses of the particles and matrix within the blades. Corrections to account for effects due to atomic number (Z), absorption (A) and fluorescence (F) within the sample, were applied. For further details of SEM and EDS experiments, see Ref. [2]. (ZAF corrections are complex, depending, amongst others, on absorption of radiation, the path scattered radiation takes and created fluorescence. These factors depend on local density and composition, and thus ZAF corrections depend on particle size, volume, shape and location in relation to the surface as well as number of particles in the zone analysed. We will make a simplifying assumption, namely that ZAF corrections for the present multiphase material can be approximated by the ZAF correction of a homogeneous system with average composition identical to the analysed composition of the multiphase material. Other work has indicated that this is a good approximation for most of the elements in MarM002 [2]. However, some deviations in the analysis in Al compositions may be expected [2].)

For assessment of the equilibrium compositions and equilibrium relative atomic fractions of the phases in MarM002 the equilibrium thermodynamics of the alloys was modelled using MTDATA [10] and THERMOCALC [11] free-energy minimisation software in conjunction with a database appropriate for Ni-base superalloys (see Ref. [12]). This database contains free-energy data of the phases that are encountered in various Ni-base superalloys as a function of composition and temperature. The free-energy minimisation software was further used to model the non-equilibrium segregation occurring on rapid cooling using the Scheil model (see e.g. Refs. [13,14,15]).

3 Results

The dendritic structure of the alloy can be revealed by optical microscopy, TEM or SEM (see Refs. [1,2,3]). In the SEM (backscattered electron imaging mode) the dendritic structure is visible as subtle differences in intensity (Fig. 1). This structure tends to become less clear on exposure at high temperature [1]. An SEM micrograph of the alloy exposed for 6000 h (250 days) at 1000ºC is presented in Fig. 2, which shows MC, M_6C and $M_{23}C_6$ carbides in addition to the γ and γ' phases identified using EDS analysis. It should be noted that isolated boride and sulphide particles may also be present in the alloy.

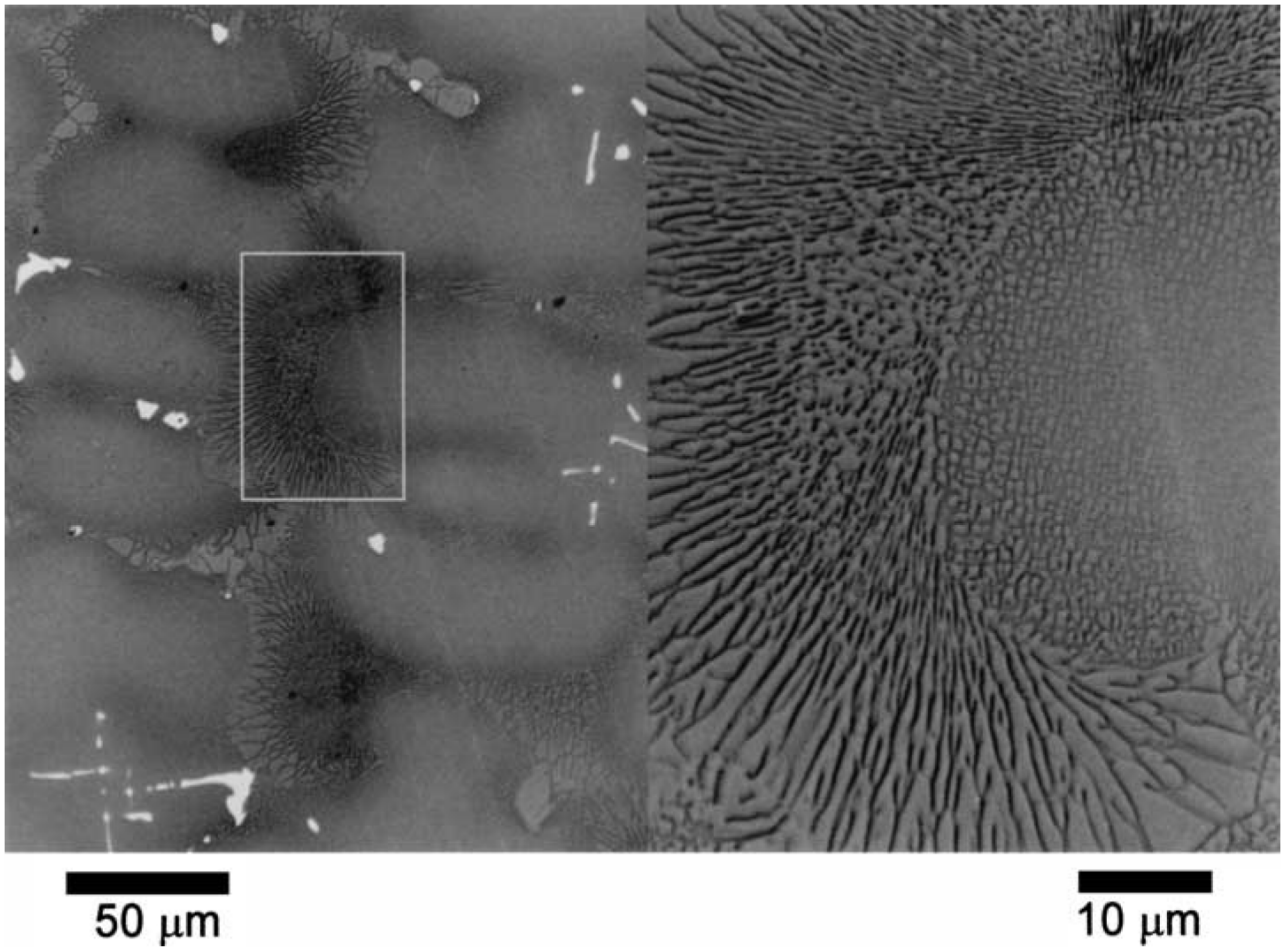

Fig. 1 SEM (back scattered electron mode) micrograph showing the dendritic structure of the as-cast MarM002 alloy. The bright particles are MC carbides, γ' phase (majority of the alloy) is light grey, γ phase is dark grey.

The dendritic segregation was analysed by performing EDS analysis on spots situated on a line perpendicular to a dendrite arm. Results presented in Fig. 3 show the variation of six alloying elements, i.e. Hf, Ta, Ti, W, Cr and Co, across dendritic structures for the as cast blades and samples exposed at 800 and 1000ºC. Minor alloying elements Fe, Zr and Mo did not show any significant variation and hence they are not presented in the figures. The Ni content was always higher in the eutectics. The figures show clear and consistent trends, compared to the gross alloy composition, Co, Cr and W contents are lower in the eutectic regions and higher in the dendrites,

and Hf, Ta and Ti contents are higher in the eutectics and lower in the dendrites. These findings reflect the fact that, compared to the gross composition, the γ phase which grows as a dendrite in the liquid has a relatively high solubility for Cr, Co and W and a low solubility for Hf, Ta and Ti. For Co, W, Hf, Ta and Ti, thermodynamic modelling of solidification with the Scheil model predicts significant segregation, consistent with the presented experimental data, but, in contrast with experimental data, this type of modelling predicts negligible Cr segregation. The latter suggests that in the temperature range where γ phase and liquid co-exist, the Cr content of the γ phase is slightly underestimated. For exposure temperatures up to 900ºC, the eutectic regions were slightly enriched in Al (difference of about 1 at%), but the enrichment increased markedly on exposure at 1000ºC (difference about 6 at%). The negative and positive signs on the x-axis represent the distance away from what are believed to be the core of the eutectics.

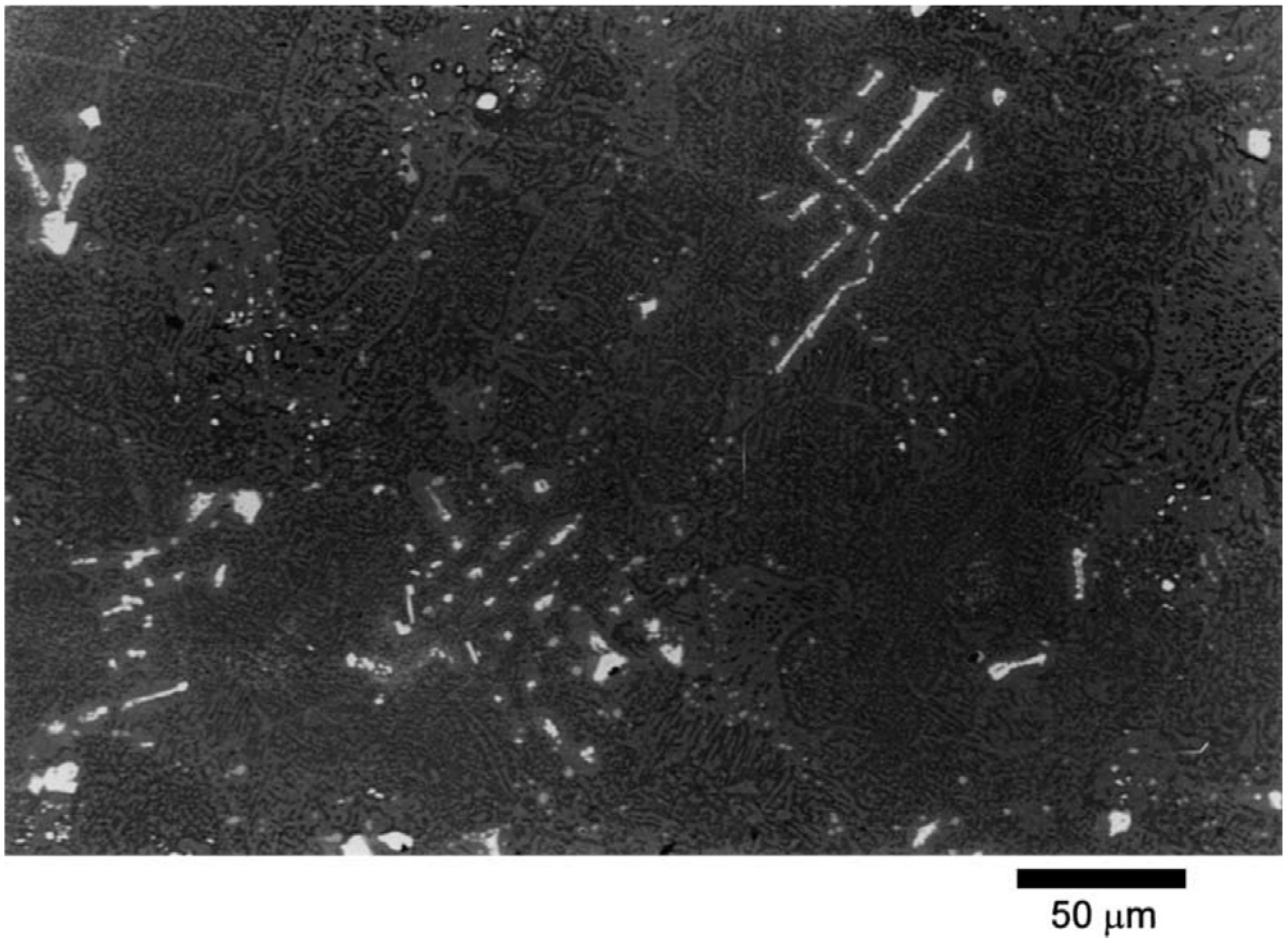

Fig. 2 SEM (back scattered electron mode) micrograph of CC MarM002 exposed for 250d at 1000ºC. The bright particles are MC and M_6C carbides, γ' phase is grey, γ phase is dark grey. The small (1 to 5 μm) light grey particles surrounded by the (somewhat darker) γ' phase are $M_{23}C_6$ carbides. Note the inhomogeneous distribution of γ' and γ phase with extended regions (30-100 μm) containing nearly exclusively γ' phase. These regions further contain most of the small (about 1 μm) Hf-rich MC particles (bright) and $M_{23}C_6$ carbides.

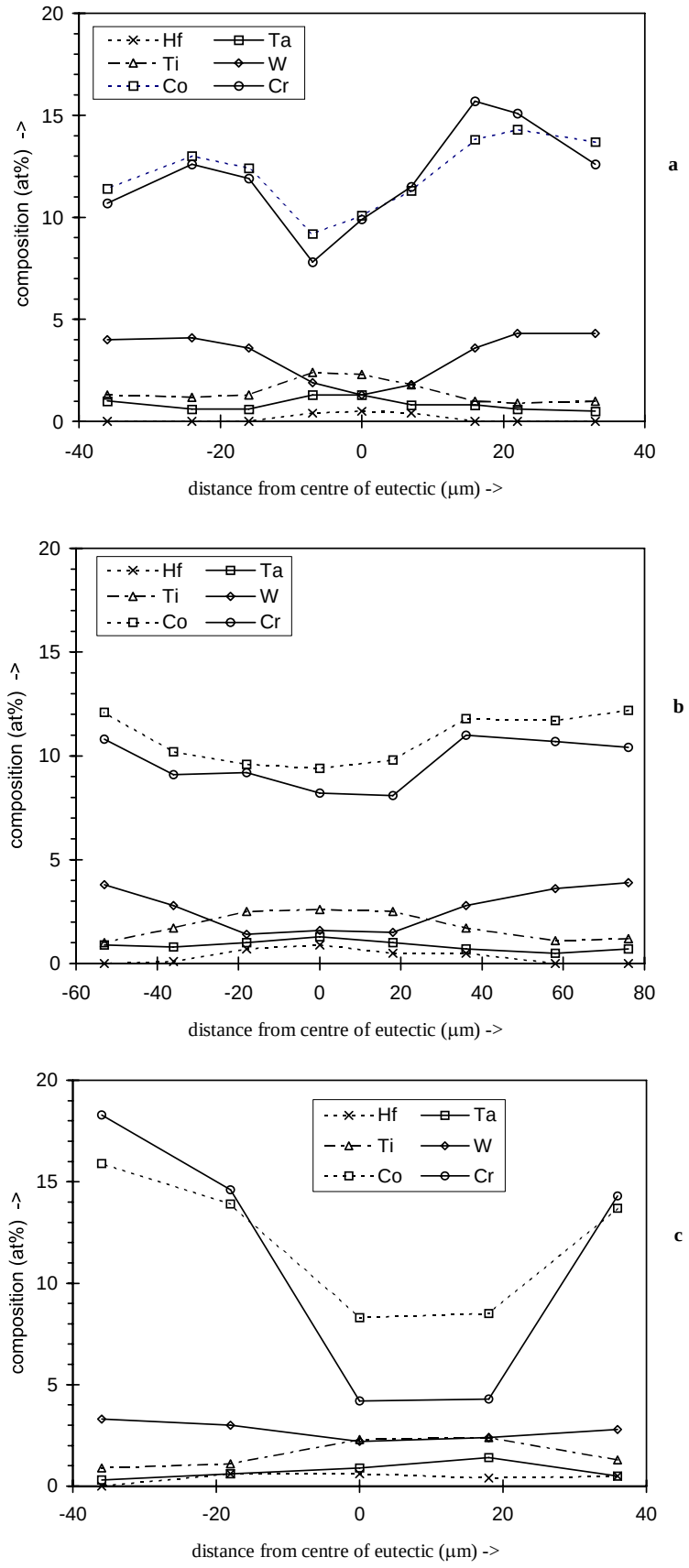

Fig. 3 Compositions measured with EDS in the SEM along a line perpendicular to a dendrite arm: a) as-cast, b) exposed 6000h at 800ºC, and c) exposed 6000h at 1000ºC.

Three experiments of the type presented in Fig. 3 were performed per sample. A complete analysis of these data confirms that consistently, and for all samples, Cr, Co and W are segregated to the dendrites while Hf, Ta and Ti are segregated to the eutectics. As the line on the surface of the SEM sample on which the EDS composition measurements are taken may cut dendrites and eutectics at different distances from their respective centres, the compositions which show maximum segregation are most representative of the composition in the centres of dendrites and eutectics. (Data from one experiment, or the average of the 3 performed per sample may not accurately reflect the maximum Cr, Co, and W content in the centres of the dendrites or the maximum Hf, Ta and Ti content in the centres of the eutectics.) Hence, attention is focused on the chemical compositions of the dendrites and eutectics which showed the maximum segregation. These data are tabulated in Table 1 and a graphical representation of the data for the two alloying elements that show the strongest tendency for segregation (Co and Cr) are presented in Fig. 4. Table 1 and Fig. 4 show that segregation in the as-cast sample is somewhat reduced as a result of commercial heat treatment, whilst further exposure at 800 and 900ºC appears to have little influence on segregation. The largest change in segregation is observed for the sample exposed at 1000ºC, which shows a much-increased segregation. This increase in segregation is most clearly observed for the major alloying elements, with Cr and Co contents in the dendrites, and Al contents in the eutectics rising to levels not encountered in other samples. This may seem rather surprising as it is generally believed that high temperature exposure reduces segregation. This finding will be explained below.

Table 1: Typical compositions (in at%) of metallic elements in dendrites and eutectic regions for CC IP MarM002 blades. For comparison also the composition of pure γ' phase in MarM002 at 900ºC as obtained in Ref. 2 is given.

Blades	Structures	Ni	Hf	Ta	W	Co	Cr	Fe	Ti	Zr	Mo	Al
as-cast	Dendrites	56.1	0.0	0.6	4.3	14.3	15.1	0.0	0.9	0.4	0.3	8.0
	Eutectics	69.3	1.8	1.5	1.5	7.9	4.5	0.0	2.9	0.5	0.2	10.0
unexposed	Dendrites	59.9	0.1	0.8	3.2	11.5	12.2	0.0	1.6	0.4	0.2	10.1
	Eutectics	65.4	0.8	0.8	1.6	9.3	8.7	0.0	2.5	0.3	0.2	10.5
800ºC	Dendrites	58.9	0.3	0.9	3.6	12.6	11.9	0	1.1	0.5	0.2	10
	Eutectics	70.7	2.0	1.5	1.3	6.5	4.3	0.2	2.9	0.8	0.2	9.7
900ºC	Dendrites	59.6	0.2	0.5	3.0	12.6	12.2	0.1	1.3	0.2	0.2	10.1
	Eutectics	65.7	1.5	1.0	1.5	9.2	7.4	0.0	2.5	0.6	0.2	10.3
1000ºC	Dendrites	53.0	0.3	0.5	3.0	16.6	20.0	0.2	0.6	0.2	0.2	5.5
	Eutectics	68.9	0.7	1.0	2.4	8.2	3.9	0.1	2.5	0.4	0.2	11.6
pure γ' in	*MarM002*	*70*	*1*	*1.1*	*2.4*	*7.2*	*3.5*	*0*	*2.7*	*0.6*	*0.2*	*11*

4 Discussion

Homogenisation of dendritic segregation proceeds by diffusion of alloying elements approximately perpendicular to the dendrite arms. The progress of this process is related to the ratio of the dendrite arm spacing (about 50 to 80 μm) and to the characteristic diffusion distances of the alloying elements in MarM002. Substantial diffusion data are only available for diffusion in pure Ni, and the characteristic diffusion distances, l ($l = 2\sqrt{D.t}$), where D is the diffusion coefficient and t is time), for Co, Cr, Al, Ti, Hf and C in Ni, are presented in Table 2. This table indicates that for the solution heat treatment at 1190ºC and the exposures at 900ºC and 1000ºC diffusion is sufficiently fast to achieve significant interaction of elements between eutectic and dendrite. However, this does not mean that this will inevitably lead to reduction of segregation, because other processes can interfere with the homogenisation process.

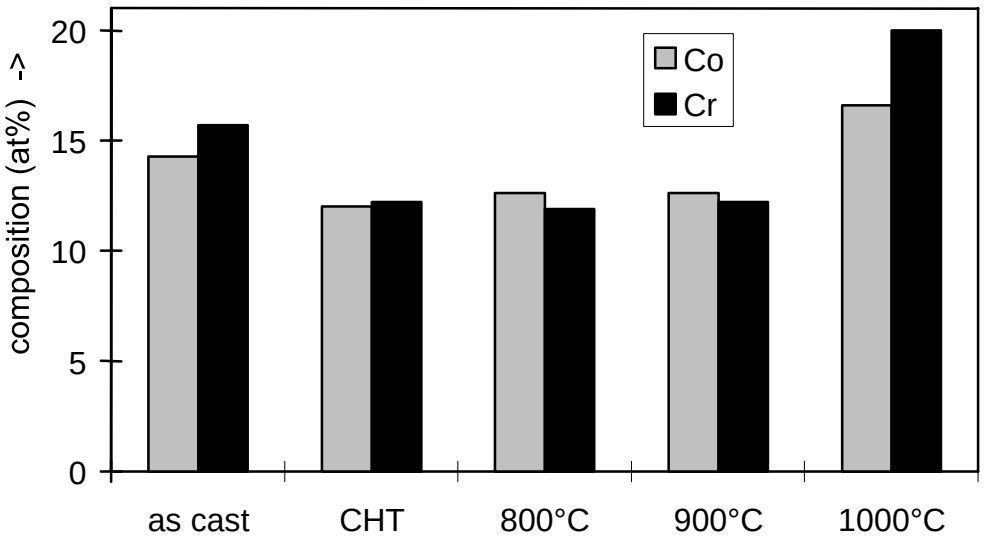

Fig. 4 Co and Cr compositions in dendrites for conventionally cast MarM002.

One example of a process that can interfere with homogenisation is the dissolution of γ' at high temperatures. This process occurs because the amount of γ' present at equilibrium decreases with increasing temperature. To assess the amount of γ' present at equilibrium the equilibrium thermodynamics of the alloys was modelled using MTDATA [10] and THERMOCALC [11] free-energy minimisation software in conjunction with a database appropriate for a (MarM002) Ni-base superalloy [12]. Results are presented in Fig. 5

Apart from compositional homogenisation and dissolution of γ' phase many other microstructural processes can occur during high temperature exposure of Ni-based superalloys. The five main types of processes are:

1. Dissolution of γ' precipitates.
2. Dissolution of MC carbides.
3. Formation of lower carbides ($M_{23}C_6$ and M_6C).
4. Coarsening of γ' precipitates.
5. Compositional homogenisation.

Each process will lower the free energy of the alloy, and therefore all of these processes can, in principle, occur. However, the extent to which they occur depends mainly on two factors:

a) the driving force for each process, i.e. the free energy reduction resulting from each process, and
b) a kinetic factor, reflecting the diffusion necessary for each process.

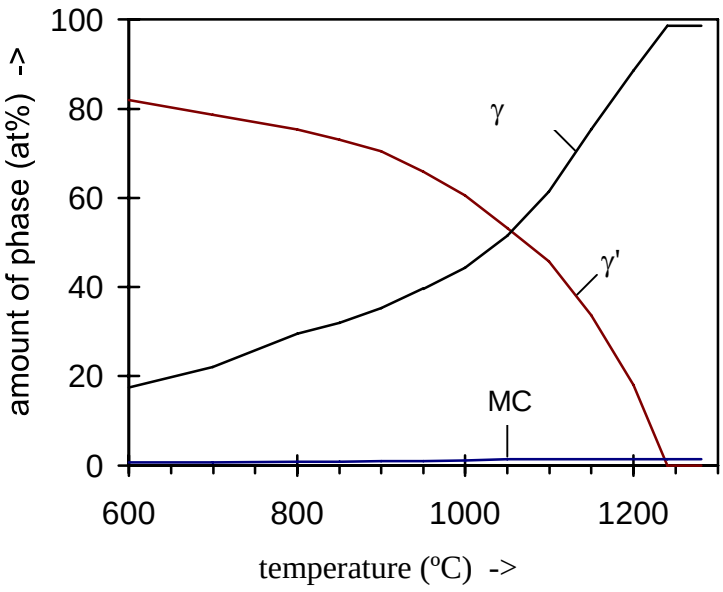

Fig. 5 Equilibrium amount of phases present in MarM002 as obtained from thermodynamic assessment.

The processes will interact and compete with each other in several, sometimes complex, ways. For instance, coarsening of γ' precipitates will compete with dissolution of γ' ($Ni_3(Al,Ti,Ta,Hf)$) precipitates which occurs because the equilibrium amount of γ' reduces with increasing temperature. In addition, both of these processes interact with dissolution of MC carbides which produces γ' following the reactions (see Ref. [1]):

$$(Ta,Ti,Hf)C + \gamma\,(Ni,Cr,Co) \rightarrow M_{23}C_6\,((Cr_{20}(W,Co,Ni)_3C_6) + \gamma'\,(Ni_3(Al,Ti,Ta,Hf))$$

$$(Ti,Ta,W)C + \gamma\,(Ni,Cr,Co) \rightarrow M_6C\,((W,Co,Ni,Cr)_6C) + \gamma'\,(Ni_3(Al,Ti,Ta,Hf))$$

Although the interactions between the processes are complex and at present difficult to model in detail, some predictions about the prevalence of the processes can be made without extensive modelling. In fact, the following semi-quantitative reasoning shows that the order in which the 5 processes are presented above is the order in which they will generally occur:

- Processes involving changes in the amount of phases will be related to the larger reductions in free energy, i.e. of the five process listed above 1-3 will have the larger driving force. (Process 4 reduces interfacial energy.)
- In the dendrites some quite fine γ' is present (TEM revealed this fine γ' with a diameter of about 0.2 μm [3]), i.e. dissolution of these precipitates (process 1) involves diffusion over distances typically less than 1 μm and can occur rapidly.
- As the solubility of carbon in γ' and γ is extremely low nearly all the carbon present in the alloy forms carbides. Thus progress of process 3, formation of lower carbides, will mainly depend on the amount of carbon released in process 2.
- Homogenisation of segregation (process 5) will involve diffusion over distances in the order of several tens of μm, coarsening of γ' (process 4) involves diffusion over much smaller distances.

Confirmation of this sequence of events can be obtained by a detailed investigation of the microstructure of exposed MarM002 using SEM as presented in Fig. 2. This figure shows evidence of the progress of processes 1-4. Firstly, there are larger areas of γ' around remnants of MC carbides, whilst lower carbides ($M_{23}C_6$ and M_6C) are detected in the vicinity (see also Ref. [1]). This demonstrates that processes 2 and 3 are occurring. Further, Fug. 2 shows large areas with relatively little γ', and some areas with nearly exclusively large and generally elongated γ'. Comparison with the as cast microstructure, whilst bearing in mind that the remnants of the elongated bright (Ta,Ti)C particles are always in the dendrites, shows that areas with nearly exclusively large, sometimes elongated, γ' are the original eutectic areas. Thus, the large areas with relatively little γ' are the original dendrites, in which originally the smaller γ' precipitates were situated. In agreement with this interpretation, the composition of the eutectic after 6000 h (250 d) at 1000ºC as presented in Table 1 is nearly equal to the composition of pure γ' (compare last two rows in Table 1).

Table 2: Diffusion distances of some relevant alloying elements in pure Ni.

	Diffusion distances (μm)			
Element	15min/1190ºC	6000h/800ºC	6000h/900ºC	6000h/1000ºC
Co	90	20	80	240
Cr	90	20	85	250
Al	130	40	150	430
Ti	140	50	160	450
Hf	270	100	320	880
C	1900	3500	6900	12300

The disappearance of the γ' phase from the dendrites as evidenced by Fig. 2 shows that the reduction of the amount of γ' phase occurs preferentially via the dissolution of the smaller γ' precipitates in the dendrites. The concentration of Co and Cr is much higher in the γ phase as compared to the γ' phase (see e.g. Ref. [2]), and therefore these observations indicate that segregation has aggravated during exposure at 1000ºC as a result of the following sequence of processes:

a) the finer γ' in the dendrites dissolves
b) some released γ' forming elements diffuse to the eutectics
c) the coarser γ' in the eutectics grows.

Note that process b involves 'uphill diffusion': some elements diffuse in the direction of increasing concentration. The driving force for this is the reduction of the average volume fraction of γ' and the increase of the average size of γ' which is achieved by dissolution of γ' precipitates in the dendrites and growth of γ' precipitates in the eutectics. It is noted that data in Table 1 do not show evidence for uphill diffusion of W, even though W is known to partition to γ. This may be explained by the fact that partitioning for W is much smaller than for Co and Cr [2]. Also, the W content is approximately one third of the Co and Cr content (in at%). Hence the driving force for uphill diffusion of W is much smaller than that for Co and Cr, which can explain the observed lack of uphill diffusion for W.)

For exposure at 800 and 900ºC much less γ' dissolution will occur with respect to that at 1000ºC (see Fig. 5), whilst γ' coarsening and long-range diffusion will be much slower and thus less extensive. Consequently, aggravation of segregation is not observed for the corresponding samples (see Table 1 and Fig. 4). The only heat treatment stage which seems to cause a reduction in segregation is solution heat treatment at 1190ºC, and also this observation can be explained in terms of the 5 main processes described above. At 1190ºC the equilibrium volume fraction of γ' is about 20vol% (see Fig. 5) and consequently treatment at (about) 1190ºC causes the finer γ' to dissolve quite rapidly leaving only the very coarse γ' undissolved. Hence after a brief period at 1190ºC there is practically no driving force for processes 1 (dissolution of γ' precipitates) and 4 (coarsening of γ' precipitates). The stability limit of $M_{23}C_6$ is about 1040ºC and little M_6C forms at 1190ºC [16], hence treatment at 1190ºC will not cause appreciable formation of lower carbides (process 3). As formation of lower carbides hardly occurs and as the solubility of C in γ phase is very low, also dissolution of MC carbide (process 2) will be limited. Thus at 1190ºC, the interference of processes 1-4 with process 5 (homogenisation) is limited and at this temperature significant homogenisation can occur.

From the above it is concluded that both the observed microstructures and the evolution of segregation of the samples is consistent with the proposed sequence of the 5 processes.

5 Conclusions

During conventional casting of MarM002, alloy dendritic segregation occurs with Cr, Co and W segregating to the dendrites and Hf, Ti and Ta segregating to the eutectics. During exposure at

1000ºC, the dendritic segregation in the CC MarM002 aggravates. This is due to the dissolution of γ' precipitates in the dendrites and coarsening of γ' precipitates in the eutectics. At temperatures up to about 1000ºC, homogenisation of dendritic segregation does not occur because it is a slow process (long diffusion distances) with a low driving force as compared to dissolution and coarsening of γ' precipitates.

Acknowledgements

The authors wish to thank Rolls Royce Industrial and Marine Gas Turbines Limited, Ansty, Coventry (UK) for providing funding for this project. The authors further wish to thank Mr. M.Z. Omar for performing part of the SEM/EDS experiments.

References

1 M.J. Starink and R.C. Thomson, unpublished research.
2 M.J. Starink M.Z. Omar and R.C. Thomson, unpublished research
3 M.J. Starink, H. Cama and R.C. Thomson, *Scr. Mater*. **38** (1997) 73.
4 C.Y. Kim, D.H. Kim, S.M. Seo, I.S. Kim, S.J. Choe and D. Knowles, Met. Mater.- Korea **6** (2000) 117
5 H.Q. Zhu, Y.J. Tang, Y.G. Li, Y.X. Zhu, Z.Q. Hu, C.X. Shi, *Mater. at High Temp.* **10** (1992) 39
6 Y. Okazaki, K. Ichikawa, M. Matsuo, *Mater. Trans. JIM* **33** (1992) 1093
7 J. Zrnik, P. Makroczy, M. Zitnansky, M. Hazlinger, *J. de Phys. IV* **3** (1993) 343
8 D.X. Ma and P.R. Sahm, *Z. Metallk.* **87** (1996) 634
9 P.K. Sung and D.R Poirier, *Metall. Mater. Trans.*. **30** (1999) 2173
10 R.H. Davies, A.T. Dinsdale, T.G. Chart, T.I. Barry and M.H. Rand, *High Temp. Sci*. **6** (1989) 251
11 B. Sundman, B. Jansson, and J.-O. Andersson, *Calphad* **9** (1985) 153
12 N. Saunders, *Phil. Trans. A* **351** (1995) 543
13 S.L. Chen, W. Oldfield, Y.A. Chang, M.K. Thomas, *Metall. Mater. Trans.* **A25** (1994) 1525
14 J.Chen, J.H. Lee, Y.S. Yoo, S.J. Choe, Y.T. Lee and B.Y. Huang, *High Temp. Mater. Proc.*. **18** (1999) 109
15 M. Rappaz and W.J. Boetinger, *Acta Mater.* **47** (1999) 3205
16 R.C. Thomson and M.J. Starink, US patent US6219404 European patent nr EP0995985